Precursor influence on the raman spectrum of $KNNLiTaLa_{0.01}$ prepared by two different methods

J. Fuentes[a], H'Linh Hmŏk[b,c,*], J. Portelles[a,d], Z. I. Bedolla-Valdez[e], J. F. Rebellón-Watson[a], R. López-Noda[a], Y. de Armas Figueroa[a], and J. M. Siqueiros[f]

[a]*Departamento de Física Aplicada, Instituto de Cibernética, Matemática y Física, CITMA, La Habana, Cuba.*
[b]*Simulation in Materials Science Research Group, Science and Technology Advanced Institute, Van Lang University, Ho Chi Minh City, Vietnam,*
[*]*e-mail: hlinhhmok@vlu.edu.vn*
[c] *Faculty of Applied Technology, School of Engineering and Technology, Van Lang University, Ho Chi Minh City, Vietnam.*
[d]*Facultad de Física, Universidad de La Habana, San Lázaro y L, La Habana 10400, Cuba.*
[e]*Tecnológico Nacional de México/ITS de Uruapan, Uruapan, Michoacán, México.*
[f]*Centro de Nanociencias y Nanotecnología, Universidad Nacional Autónoma de México, Apartado Postal 14, Ensenada 22860, Baja California, México.*

Received 1 June 2023; accepted 1 November 2023

This work presents a study of ceramics with the $(K_{0.44}Na_{0.52}Li_{0.04})_{0.97}La_{0.01}Nb_{0.9}Ta_{0.1}O_3$ composition through their Raman spectra. In previous studies [1], this composition has shown good permittivity and piezoelectric parameter values that justify a deeper investigation. Two sets of samples of these ceramic compounds were prepared using different methods. The first set was prepared using a classical solid-state reaction of oxides and carbonates, as described in Ref. [2]. The second set was prepared using the $NaNbO_3$ precursor. The Raman spectra of the samples obtained by the direct ceramic method consisted of 5 modes. In contrast, the spectra of the samples obtained using the precursor showed a shift of the wavenumber of the $A_{1g}(\nu 1)$ mode peak towards lower values and consisted of seven modes with the appearance of two additional modes, $F_{1u}(\nu 3)$ and $F_{2g}(\nu 4)$. Notably, using the precursor preparation route led to important improvements with a more straightforward method than Saito *et al*. [3].

Keywords: Raman spectroscopy; lead-free piezoelectrics; solid-state reaction; RTGG.

DOI: https://doi.org/10.31349/RevMexFis.70.021601

1. Introduction

The doping of $K_{0.5}Na_{0.5}NbO_3$ (KNN) piezoceramics with different elements such as Li, La, and Ta is used to move the transition temperature of the tetragonal (T) to orthorhombic (O) phase toward room temperature, that is, the Polymorphic Phase Transition (PPT), where the properties of the piezoceramics are enhanced. The doping with La has the effect of lowering the O-T transition temperature as well as the Curie temperature [4], while doping with Li increases the Curie temperature but diminishes the O-T transition temperature [5–7]. Doping with Li, La, and Ta further enhances the shift of the ferroelectric-paraelectric transition temperature, as characterized by the Curie temperature (T_C), where the crystalline symmetry of KNN changes from tetragonal to cubic. Such complex doping is necessary to obtain the KNN piezoceramic values of the parameter d_{33} and the permittivity as high as those in the lead zirconate titanate (PZT) piezoceramics. There are different issues to solve in the KNN piezoceramic, such as the dependence of the morphotropic phase transition on temperature and the loss of Potassium (K) and Sodium (Na) during the sintering of the piezoceramics. The doping of piezoceramics causes changes in the crystal structure, and the apparition of defects affects the response of the cell, and those changes can be seen in the Raman spectra. For this reason, Raman Spectroscopy is used in the studies of these piezoceramics. The intensity and the wavenumbers of the characteristic Raman modes depend, to a certain degree, on the presence of defects that affect the vibration modes of the oxygen octahedra [4, 8–10].

The study of compositions that differ only in using the $NaNbO_3$ precursor was motivated by the search for alternatives to obtain high dielectric permittivity values and k_{31} coefficient values. We found that the dielectric permittivity with a value of 6800 with minimum dielectric losses was the highest achieved in KNN ceramics. Dielectric measurements show that La and Li doping reduces the transition temperatures compared to those of undoped KNN (tetragonal-cubic T_{T-C} = 264°C and orthorhombic-tetragonal T_{O-T} = 90°C). Hysteresis loop obtained by PFM shows an effective piezoelectric coefficient d_{eff} = 164 pC N^{-1}, comparable to the best values of PZT and KNN ceramics. However, the reason underlying this study is the fact that the improved piezoelectric properties of the compound are strongly related to tex-

ture. The goal is to produce platelet shaped grains. That is why the material obtained through the $NaNbO_3$ precursor performs better. This preparation technique favors obtaining platelet shaped grains similar to those obtained by Saito *et al*. [3] in his seminal research, but with a simpler preparation method. Saito *et al*. [3] achieved outstanding piezoelectric parameter values in $(K_{0.44}Na_{0.52}Li_{0.04})(Nb_{0.86}Ta_{0.1}Sb_{0.04})O_3$ piezoceramics by using a variant of the reactive-templated grain growth technique. Similarly, in the present work, the $KNNLiTaLa_{0.01}$ samples obtained using the $NaNbO_3$ precursor with our two-step method show exceptional values of the permittivity and d_{33} parameter as reported in Ref. [1], attributed to the activation of the $F_{1u}(\nu 3)$ and $F_{2g}(\nu 4)$ Raman modes.

2. Experimental

Ceramics with $(K_{0.44}Na_{0.52}Li_{0.04})_{0.97}La_{0.01}Nb_{0.9}Ta_{0.1}O_3$ ($KNNLiTaLa_{0.01}$) composition were prepared in two ways, first by solid-state reaction of oxides and carbonates: K_2CO_3 (99.0%, FagaLab), Na_2CO_3 (99.0%, FagaLab), La_2O_3 (99.99%, metal Basic, Alfa Asear), Nb_2O_5 (99.9%, metal Basic, Alfa Aesar), Li_2CO_3 (99.0%, FagaLab) and Ta_2O_5 (99.0%, FagaLab) as was described in Ref. [2]. The sintering process was performed at 1200°C under a controlled atmosphere in sealed crucibles covered with $KNNLiTaLa_{0.01}$ powders to prevent the loss of volatile components. In the second method, a two-step procedure, the $NaNbO_3$ precursor was synthesized from the topochemical reaction between $Bi_{2.5}Na_{3.5}Nb_5O_{18}$ (BiNN) and Na_2CO_3, using the Reactive-Templated Grain Growth Method. The obtained precursor was then made to react through a solid-state reaction with the same reactants at the sintering temperature of 1200°C, in a controlled atmosphere [1]. This combined method uses the precursor as a seed so that the resultant compound grows on the structure and with the orientation of the $NaNbO_3$ precursor. The crystal structure of the samples was determined by X-ray diffraction (XRD) using a Philips X'pert diffractometer with CuKα radiation from 10° to 90° in 2θ, 0.02° step and exposition time of 0.5 s, at 30 kV and 16 mA. Micro-Raman measurements were performed in a Labram Dilor Microraman, with a 10 mW Ar^+ laser with λ = 514 nm emission wavelength.

3. Results and discussion

3.1. XRD measurements

For both patterns, corresponding to the sample prepared without the use of the precursor, labeled MX11 [Fig. 1a)] and the sample obtained using the precursor labeled TEX04 [Fig. 1b)], the fitting was based on a mixture of an orthorhombic perovskite phase of the Amm2 space group and a tetragonal perovskite of the P4mm space group. Reflections associated with a spurious phase (tungsten-bronze phase) are also present. Lattice parameters are presented in Table I for the MX11 sample [2] and in Table II for the TEX04 sample.

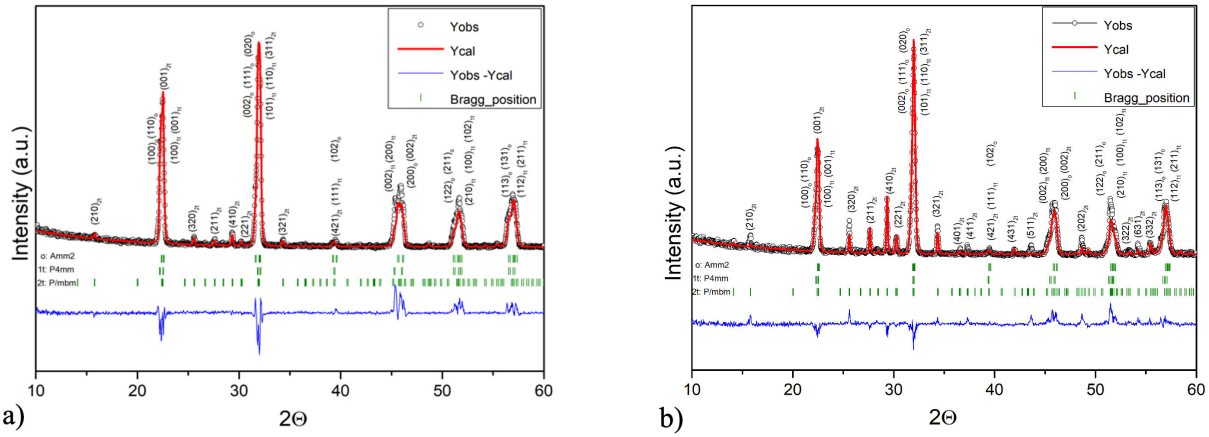

FIGURE 1. XRD pattern corresponding to the a) MX11 sample obtained without the $NaNbO_3$ precursor [2], and b) TEX04 sample obtained using the $NaNbO_3$ precursor.

TABLE I. Phases present, space group, lattice parameters (Å) and sample percentage content without using the precursor (MX11).

Sample	Phases present	Space Group	Lattice parameters(Å)			Percentage content (%)
			a	*b*	*c*	
MX11	Tetragonal	P4mm	3.945(2)	3.945(2)	4.005(2)	46.08
	Orthorhombic	Amm2	3.936(3)	5.584(4)	5.656(4)	45.26
	Tetragonal	P4bm	12.554(9)	12.554(9)	3.953(6)	8.66

Conventional Rietveld Rp, Rwp, Re and Chi^2: 25.1, 25.0, 19.1 and 1.71

TABLE II. Phases present, space group, lattice parameters (Å) and percentage content of the sample obtained using the precursor (TEX04).

Sample	Phases present	Space Group	Lattice parameters(Å)			Percentage content (%)
			a	b	c	
TEX04	Tetragonal	P4mm	3.952(5)	3.952(5)	3.986(5)	66.12
	Orthorhombic	Amm2	3.934(6)	5.586(1)	5.611(2)	13.57
	Tetragonal	P4bm	12.5598	12.5598	3.9444	22.01

Conventional Rietveld Rp, Rwp, Re and Chi^2: 26.7, 27.1, 24.0 and 1.272

3.2. Raman measurements

Figures 2a) and 2b) show the Raman spectra from 100 to 700 cm^{-1}, corresponding to the normal vibrational modes of the (Nb/Ta)O_6 oxygen octahedra of the MX11 and TEX04 samples at 20°C, respectively. The Raman spectra were fitted using a LabSpec 6-HORIBA Scientific software by the GaussLor () method. The baseline of all spectra was subtracted before the fitting; twenty iterations and a maximum shift of 5 cm^{-1} were considered. For the 100-700 cm^{-1} region, the spectra were fitted with five GaussLor peaks for the MX11 sample and seven for the TEX04 sample. The modes were identified using previously published works on Raman spectroscopy of KNN based materials as reference [6,11–13]. The wave number values and intensity for the Raman spectra of the MX11 and TEX04 samples are presented in Tables III and IV, respectively. After the corresponding fitting process, $F_{2u}(\nu 6)$, $F_{2g}(\nu 5)$, $F_{2g}(\nu 4)$, $E_g(\nu 2)$, $F_{1u}(\nu 3)$ and $A_{1g}(\nu 1)$ vibrational normal modes were identified and a small band corresponding to the spurious Tetragonal Tungsten Bronze (TTB) phase [6, 11–13], where $A_{1g}(\nu 1)$, $E_g(\nu 2)$ and $F_{1u}(\nu 3)$ are stretching modes, and $F_{2g}(\nu 5)$, $F_{2g}(\nu 4)$ and $F_{2u}(\nu 6)$ are bending modes [10, 12, 13]. The $F_{1u}(\nu 3)$ y $F_{2g}(\nu 4)$ modes in the Raman spectra are not reported in the articles on non-doped KNN and doped KNN with Li and La [2, 4, 8, 10, 12, 13].

Since no differences in the XRD patterns of both samples are observed, we conclude that the presence of these modes is caused by the use of the precursor obtained by the RTGG method in preparing the sample that causes alterations in the (Nb/Ta)O_6 octahedra. Additionally, the XRD patterns of the TEX04 sample do not show the same texture as those observed in the XRD patterns of Saito et al. [13].

The MX11 XRD pattern shows the same phase composition, the only difference being the presence of traces of a tungsten bronze secondary phase due to the shorter sintering process time. However, these structural alterations attributed to the precursor were not detected in the XRD patterns. The activation of the $F_{1u}(\nu 3)$ y $F_{2g}(\nu 4)$ modes is due to the presence of polarization vectors perpendicular to the basal plane as determined from the PFM micrographs. This is the reason for the exceptional values of permittivity and d_{33} parameter in the TEX04 sample [1], that is, through the activation of the $F_{1u}(\nu 3)$ y $F_{2g}(\nu 4)$ modes associated with oscillations in the plane perpendicular to the basal plane of the structure, as can be seen in the graphs of the KNN modes in Refs. [10,11] and measured by PFM [1].

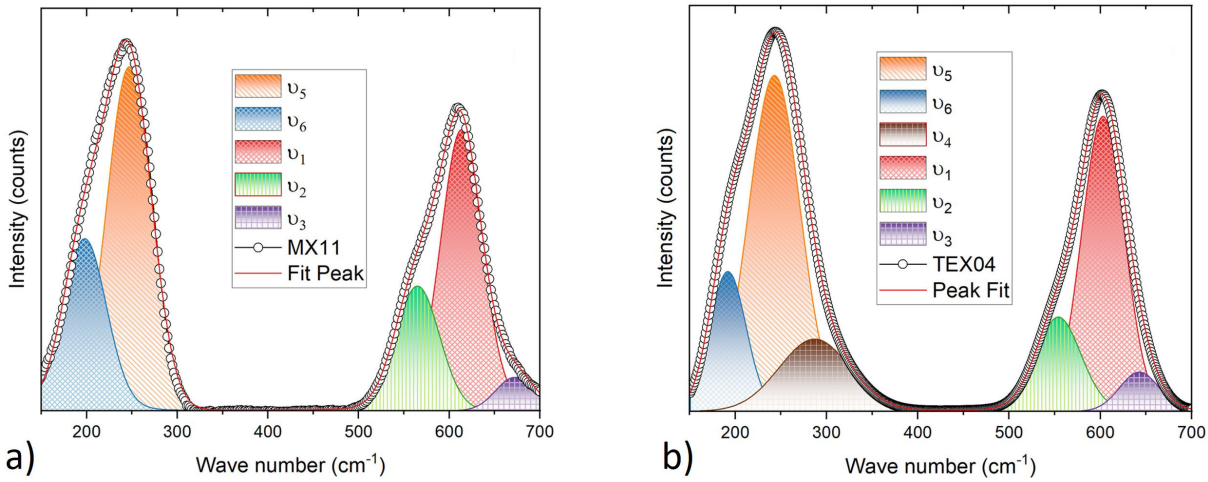

FIGURE 2. Adjusted Raman spectrum for the a) MX11 sample with χ^2=0.0626, and b) TEX04 sample with χ^2=0.0088.

TABLE III. The wave number values and intensity for the Raman spectrum of the MX11 sample.

Modes	$F_{2u}(\nu_6)$		$F_{2g}(\nu_5)$		$E_g(\nu_2)$		$A_{1g}(\nu_1)$		$F_{1u}(\nu_3)$	
Sample	Wave No.	Intensity	Wave No.	Intensity	Wave No.	Intensity	Wave No.	Intensity	Wave No.	Intensity
MX11	197.78	0.46	247.08	0.93	564.94	0.34	613.31	0.76	672.28	0.09

TABLE IV. The wave number values and intensity for the Raman spectrum of the TEX04 sample.

Modes	$F_{2u}(\nu_6)$		$F_{2g}(\nu_5)$		$F_{2g}(\nu_4)$		$E_g(\nu_2)$		$A_{1g}(\nu_1)$		$F_{1u}(\nu_3)$+TTB	
Sample	Wave No.	Intensity	Wave No.	Intensity	Wave No.	Intensity	Wave No.	Intensity	Wave No.	Intensity	Wave No.	Intensity
TEX 04	191.87	0.37	242.93	0.88	287.0	0.19	554.0	0.25	603.0	0.078	642.8	0.23

Doping KNN with Li, La at the A site of the perovskite structure distorts the (Nb/Ta)O_6 octahedra. It shifts the orthorhombic-to-tetragonal (O-T) phase transition temperature (T_{O-T}) of $K_{0.5}Na_{0.5}NbO_3$ towards room temperature (RT). The shift is accompanied by a decrease in the wavenumber of the $A_{1g}(\nu 1)$ mode peak. This behavior is observed in Tables III and IV, where the $A_{1g}(\nu 1)$ mode peak is at a lower wave number than that of the orthorhombic phase placed at 614 cm^{-1} [2, 4]. The shift towards lower wave numbers results from doping with La^{+3} y Li^{+1}, which have smaller ionic radii than K^+ and Na^+. This increases the distance between A ions and the coordinated oxygens, reducing the force constant and modifying the oscillation frequencies.

In the case of the TEX04 sample, seven bands are observed, and in the band corresponding to the $F_{1u}(\nu_3)$ an overlap is observed with the band corresponding to the TTB phase in 642.8 cm^{-1}. It is shown, by the values of the dielectric permittivity, the importance of the presence of the tungsten bronze phase to achieve high values of dielectric permittivity in ceramics of the type of $KNNLiTaLa_{0.01}$. Everything seems to indicate that the precipitation in a coherent way of the TTB phase ensures the high values of the dielectric permittivity. The use of the $NaNbO_3$ precursor and the precipitation of the bronze tungsten phase determines the obtainment of the very high values of the Dielectric Permittivity in the TEX04 sample (Table V).

TABLE V. Sintering temperatures (°C) and Dielectric Permittivity (ϵ_r) of different samples.

Sample	Sintering temperature	TT phase	ϵ_r
MX01	1150	no	1540
MX13	1180	no	1627
MX11	1200	yes	1961
TEX04	1200	yes	6800

4. Conclusions

This work presents a study of ceramics with the $(K_{0.44}Na_{0.52}Li_{0.04})_{0.97}La_{0.01}Nb_{0.9}Ta_{0.1}O_3$ composition through their Raman spectra. These ceramics were prepared using two methods: a classical solid-state reaction of oxides and carbonates, and a two-step procedure involving the synthesis of the $NaNbO_3$ precursor using the Reactive-Templated Grain Growth (RTGG) method. The obtained precursor was then reacted with appropriate carbonates and oxides through a solid-state reaction to obtain the desired composition. The Raman spectra of the samples obtained by the ceramic method consisted of five modes, while the spectra of the samples obtained by the two-step method consisted of seven modes with the appearance of two new modes, $F_{1u}(\nu 3)$ and $F_{2g}(\nu 4)$. Although this structural alteration attributed to the precursor was not detected in the XRD patterns, the activation of the $F_{1u}(\nu 3)$ and $F_{2g}(\nu 4)$ modes, associated with oscillations in the plane perpendicular to the basal plane of the structure, led to exceptional values of the permittivity and d_{33} parameter in the TEX04 sample. The doping of KNN with Li and La at the A site of the perovskite structure distorts the (Nb/Ta)O_6 octahedra and induces a shift of the wave number of the $A_{1g}(\nu 1)$ mode peak towards lower values. This shift is a consequence of the presence of the tetragonal phase at room temperature due to doping with Li and La reducing the force constant and, consequently, modifying the oscillation frequencies.

Acknowledgements

One of the authors thanks PAPIIT-DGAPA-UNAM for partial support of this work through Grant No. IN103323. H'Linh Hmŏk acknowledges the support of Van Lang University. M. A. Hernández and C. Ostos acknowledge for the calculations.

1. J. Portelles *et al.*, Li, La, Ta doped KNN ceramics obtained by RTGG, *Ferroelectrics* **534** (2018) 175-182.
2. J. Fuentes *et al*., Physical properties of the $(K_{0.44}Na_{0.52}Li_{0.04)})_{0.97}La_{0.01}Nb_{0.9}Ta_{0.103}$ ceramic with coexisting tetragonal and orthorhombic monocrystalline grains at room temperature. *Ceram. Int.* **47** (2021) 11958-11965.
3. Y. Saito *et al*., Lead-free piezoceramics, *Nature* **432** (2004) 84.
4. X. Vendrell *et al*., Effect of lanthanide doping on structural, microstructural and functional properties of $K_{0.5}Na_{0.5}NbO_3$ lead-free piezoceramics, *Ceram. Int.* **42** (2016) 17530-17538.
5. J. Fuentes *et al.*, Structural and dielectric properties of La and Ti modified K0.5Na0.5NbO3 ceramics, *Appl. Phys. A* **107** (2012) 733-738.
6. J. Li *et al*., (K,Na) NbO_3-based lead-free piezoelectric: fundamental aspect, processing Technologies, and remaining challenges, *J. Am. Ceram. Soc*. **96** (2013) 3677-3696.
7. X. Sun *et al*., Effects of Li Substitution on the Structure and Ferroelectricity of (Na,K)NbO3, *J. Am. Ceram. Soc*. **92** (2009) 3033-3036.
8. N. Klein *et al.*, A study of the phase diagram of (K, Na, Li)NbO_3 determined by dielectric and piezoelectric measurements, and Raman spectroscopy, *J. Appl. Phys.* **102** (2007) 014112.
9. Giuseppe Pezzotti, Raman Spectroscopy of piezoelectrics, *J. Appl. Phys.* **113** (2013) 211301
10. K. Kakimoto et al., Raman Scattering Study of Piezoelectric $(Na_{0.5}K_{0.5})NbO_3$-$LiNbO_3$ Ceramics, *Jpn. J. Appl. Phys*. **44** (2005) 7064-7067.
11. Y. de Armas Figueroa *et al*., Study of a polymorphic phase transition in KNNLiTaLa0.01 by Raman spectroscopy, *Phase Transitions* **95** (2022) 1-8. 9
12. F. Rubio-Marcos *et al.*, Correlation between the piezoelectric properties and the structure of lead-free KNN-modified ceramics, studied by Raman Spectroscopy, *J. Raman Spectrosc.* **42** (2011) 639-643.
13. F. Rubio Marcos *et al.*, Resolution of the ferroelectric domains structure in (K,Na)NbO3- based lead-free ceramics by confocal Raman microscopy, *J. Appl. Phys.* **113** (2013) 187215.